ORIGINAL PAPER

A simple sensor based on 1-butylpyridinium hexafluorophosphate@ glassy carbon microspheres composites for the quantitative analysis of azo dyes

Yonghong Li[1,2] · Yutong Li[1] · Leina Jia[1] · Yuan Li[1] · Yan Wang[1] · Pengju Zhang[1] · Xinsheng Liu[3]

Abstract

The overuse of synthetic colorants may result in hepatocellular damage, renal failure, and potential immunotoxicity. Therefore, the content of synthetic colorants in foods must be strictly controlled. A simple sensor based on 1-butylpyridinium hexafluorophosphate@glassy carbon microspheres composites electrode (GCILE) was constructed for the rapid and sensitive detection of sunset yellow (SY) and tartrazine (TZ). Composite materials were investigated using scanning electron microscopy and Fourier transform infrared spectroscopy. Then the electrochemical properties of the sensors were characterized using cyclic voltammetry. Furthermore, the electrochemical behaviors of SY and TZ were studied at the GCILE using differential pulse voltammetry. The effects of pH value, the different ratios of glassy carbon microspheres and ionic liquid, accumulation time, and accumulation potential on current responses of SY and TZ were discussed in detail. The GCILE displayed favorable electrocatalytic activity to SY and TZ. Under the optimum experimental conditions, the linear ranges of SY and TZ were 0.02–5 µM and 0.5–15 µM, respectively. When the noise–signal ratio (S/N) was 3, the detection limits of SY and TZ were 0.01 and 0.1 µM, respectively. Interference studies showed that common interfering substances did not affect the detection of SY and TZ. The proposed method was applied for analyzing azo dyes in beverages.

Keywords Sunset yellow · Tartrazine · Glassy carbon microspheres · Ionic liquid · Differential pulse voltammetry

Introduction

Synthetic colorants are widely used in the food industry due to their low price, good color uniformity, high stability, and low microbiological contamination. Synthetic colorants are generally classified into azo, triarylmethane, quinolone, xanthene, and indigoid compounds [1]. Sunset yellow (SY) and tartrazine (TZ), as two common synthetic azo dyes, are widely used in candies, drinks, and dairy products. Recent studies show that excessive or prolonged consumption of SY and TZ can cause eczema, allergies, asthma, childhood hyperactivity, and even cancer [2–4]. Therefore, the content of azo dyes in food should be strictly controlled. The simple, rapid, and sensitive analysis of these dyes is crucial for food safety.

Various methods have been utilized to analyze synthetic food colorants, such as spectrophotometry [5], high-performance liquid chromatography [6], thin-layer chromatography [7], capillary electrophoresis [8], and electrochemical methods [9, 10]. Compared with other analytical techniques, electrochemical methods exhibit the advantages of low cost, fast response, and high sensitivity.

Carbon paste electrode (CPE) usually consists of paraffin oil and graphite powder. CPE can be simply prepared with a low background current, and the electrode surface is easily renewable [11]. Various carbon materials and binders with excellent properties have replaced graphite powder and paraffin oil to improve the performance of CPE. For example, Keyvanfard et al. [12] described the application

✉ Yonghong Li
yonghongli2012@163.com

✉ Xinsheng Liu
lxs21230@163.com

1 School of Public Health and Management, Ningxia Medical University, Yinchuan 750004, People's Republic of China

2 Key Laboratory of Environmental Factors and Chronic Disease Control, Yinchuan 750004, People's Republic of China

3 School of Basic Medical Sciences, Ningxia Medical University, Yinchuan 750004, People's Republic of China

of multiwall carbon nanotubes paste electrode for penicillamine (PA) determination in the presence of chlorpromazine. The sensor exhibited very efficient electrocatalytic activity to PA. Mohammadi et al. [13] used the modified graphene oxide nanosheets paste electrode to detect epinephrine and uric acid. Motoc et al. [14] prepared a fullerene–carbon nanofiber paste electrode, and the modified electrode showed the enhanced electrochemical response of diclofenac. Li et al. [15] described a nanocarbon ionic liquid electrode modified with palladium-doped graphene. The peak currents of dopamine and uric acid were increased and their peak potentials were reduced on the prepared electrode compared with CPE.

Recently, glassy carbon paste electrode (GCPE) has been constructed on the basis of CPE. It is constructed by using glassy carbon microspheres instead of graphite powder. It exhibits high electrochemical reactivity and a wide potential window. Several sensors based on GCPE have been reported. Ören et al. [16] used a gold nanoparticle–glassy carbon paste composite electrode for fast and sensitive analysis of caffeine. Dai et al. [17] prepared a glassy carbon microspheres and ionic liquid composite paste electrode as a new electrochemiluminescent sensor, which was sensitive to fentanyl citrate.

In this work, we utilized glassy carbon microspheres instead of graphite powder and the ionic liquid 1-butylpyridinium hexafluorophosphate as binds to fabricate composites electrodes. The modified electrode was constructed in a simple preparation procedure, and it was first used to detect SY and TZ simultaneously. The proportions of glassy carbon microspheres and ionic liquid were optimized, and the property of the modified electrode was greatly improved. The modified electrode showed excellent electrochemical activities to SY and TZ, resulting in increased oxidation currents. The suggested method was successfully applied to the analysis of SY and TZ in beverages.

Experimental

Reagents and materials

Glassy carbon microspheres (particle size: 2–12 μm), sunset yellow, and tartrazine were obtained from Sigma-Aldrich. The ionic liquid 1-butylpyridinium hexafluorophosphate (BPPF$_6$) was acquired from Lanzhou Institute of Chemical Physics. Paraffin oil and graphite powder (spectrographic grade) were purchased from Sinopharm Chemical Reagent Co., Ltd. (Shanghai, China). 0.1 M phosphate buffer solution (PBS) was made up of Na$_2$HPO$_4$ and KH$_2$PO$_4$.

Apparatus

Electrochemical measurements were operated on a CHI660E electrochemical workstation (Shanghai Chenhua Instruments Corporation, shanghai, China). A three-electrode system was utilized containing a 1-butylpyridinium hexafluorophosphate@glassy carbon microspheres composite electrode (GCILE) (3.0 mm in diameter), a platinum wire, and a saturated calomel electrode (SCE). A Hitachi S-3400 scanning electron microscope was used to acquire scanning electron micrographs (Hitachi Ltd., Tokyo, Japan). The Fourier transform infrared spectra were recorded by IR Affinity-1 infrared spectrometer (Shimadzu Co., Japan). Ultrapure water (18.2 MΩ cm) was prepared by an ultrapure water system (Heal Force NW 30VFE). The testing solution was stirred before measurements using a KMO2 magnetic stirrer (IKA, Germany).

Electrode preparation

Firstly, different proportions of glassy carbon microspheres (GC) and ionic liquid (IL) were added and hand-mixed in an agate mortar. Then the mixture was filled firmly into the cavity of a Teflon holder (3.0 mm in diameter), and the electrical contact was built by copper wire. A hair drier was employed to heat the electrode until the binder 1-butylpyridinium hexafluorophosphate fully melted. A smooth surface could be obtained by polishing the modified electrode on a piece of weighing paper. The prepared electrode above was 1-butylpyridinium hexafluorophosphate@glassy carbon microspheres composites electrode, which was denoted as GCILE.

For comparison, graphite powder and ionic liquid were used to prepare carbon ionic liquid electrode (CILE). Glassy carbon microspheres paste electrode (GCPE) was constructed with paraffin oil and glassy carbon microspheres. Traditional carbon paste electrode (CPE) was made up of paraffin oil and graphite powder.

Analytical procedure

The electrochemical properties of modified electrodes were studied in 1 mM Fe[(CN)$_6$]$^{3-/4-}$ and 0.1 M KCl solution using cyclic voltammetry (CV). SY and TZ were analyzed using differential pulse voltammetry (DPV). The accumulation step and determining step were two main steps in the analysis process. Firstly, SY and TZ were preconcentrated onto the GCILE surface under 0.5 V for 150 s stirring. Secondly, DPV signals of SY and TZ were measured from 0.3 to 1.1 V. The fabrication procedure of the GCILE and electrochemical analysis of SY and TZ is presented in Scheme 1.
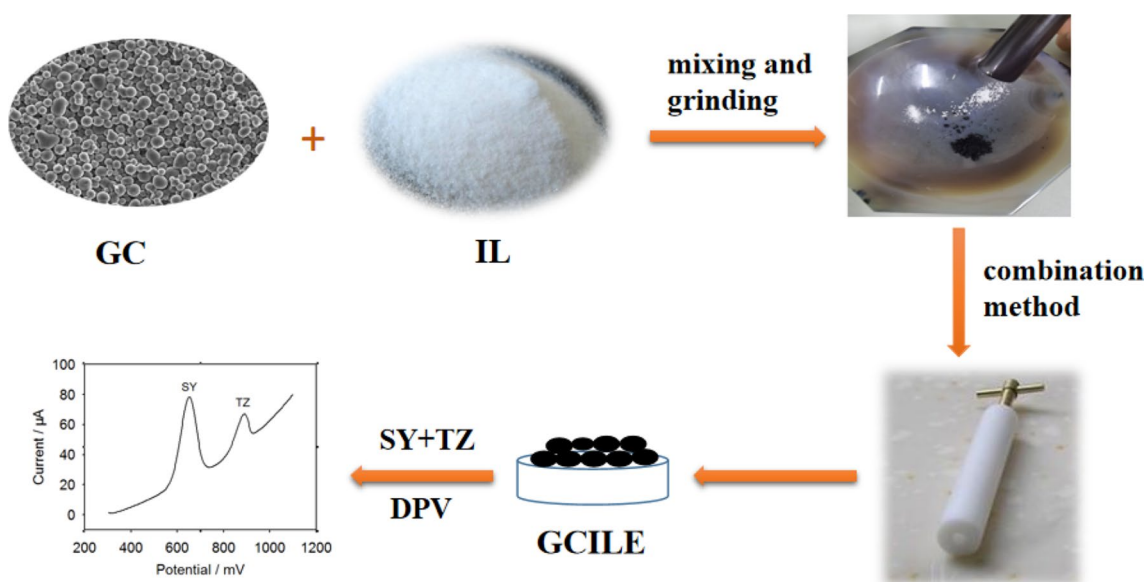
Scheme 1 Fabrication procedure of the GCILE and electrochemical analysis of SY and TZ

Results and discussion

Surface morphologies and structures characterization

The surface morphologies of GCPE and GCILE were investigated using scanning electron microscopy. Large gaps between glassy carbon microspheres were observed on the GCPE in Fig. 1a. However, Fig. 1b clearly showed that GCILE exhibited a compact and uniform surface. Compared with GCPE, the ionic liquid instead of paraffin oil was used as the binder for the construction of GCILE. The interstices between microspheres were filled with highly viscous ionic liquids, forming a unified whole.

FT-IR spectroscopy was performed to identify the chemical groups of GC and GC-IL hybrids. The infrared spectra of GC and GC-IL are presented in Fig. 1c. Many absorption signals were matched between the two spectra. Because CO_2 in the air was adsorbed during the sample test, weak absorption peaks were observed between 2250 and 2500 cm^{-1} in Fig. 1c (curves a and b). The FT-IR spectrum of the GC-IL hybrids (curve b) revealed absorption peaks of $BPPF_6$. The absorption peaks located between 1410 and 1700 cm^{-1} indicated the characteristic peaks of the pyridine ring (containing the stretching vibrations of C=N and C=C in the pyridine ring). The peaks appeared at 3152 and 3107 cm^{-1} corresponded to C-H on the pyridine ring. The peaks located at 2974, 2942, and 2885 cm^{-1} were attributed to the stretching vibrations of C-H on the alkyl chain. Due to PF_6^- stretching vibration, the absorption peak was found at 835 cm^{-1}. The results above clarified that the ionic liquid $BPPF_6$ was successfully combined with GC.

Electrochemical characterization

The electrochemical performances of the modified electrodes were discussed using cyclic voltammetry (CV). Figure 2 shows the CVs of different electrodes in 1 mM $[Fe(CN)_6]^{3/4-}$ and 0.1 M KCl solution. The weak redox peaks appeared on the CPE (Curve a). A pair of well-defined redox peaks was observed on CILE (Curve b). The ionic liquid acted as a charge transfer bridge on the electrode surface and improved electron transfer kinetics. As the graphite powder was replaced by glassy carbon microspheres, the peak currents increased obviously, and the peak–peak potential difference was reduced on GCILE (Curve c). The improved electrochemical performance of the GCILE was probably ascribed to the high conductivity of the ionic liquid and the large surface area of glassy carbon microspheres.

Surface area study

The electroactive surface areas of CILE and GCILE were investigated in $K_3[Fe(CN)_6]$ redox system, and the results are shown in Fig. 3. According to Randles–Sevcik equation [18], the anodic peak current (I_{pa}) was proportional to square root of scan rate ($\nu^{1/2}$) for a reversible process:

$$I_{pa} = \left(2.69 \times 10^5\right) n^{3/2} A C_0 D_R^{1/2} \nu^{1/2} \qquad (1)$$

where I_{pa} corresponds to anodic peak current, n stands for electron transfer number (n = 1), A refers to the electroactive surface area (cm^2), C_0 is the concentration of $K_3[Fe(CN)_6]$ (1 mM), and D_R and ν are the diffusion coefficient (7.6×10^{-6}
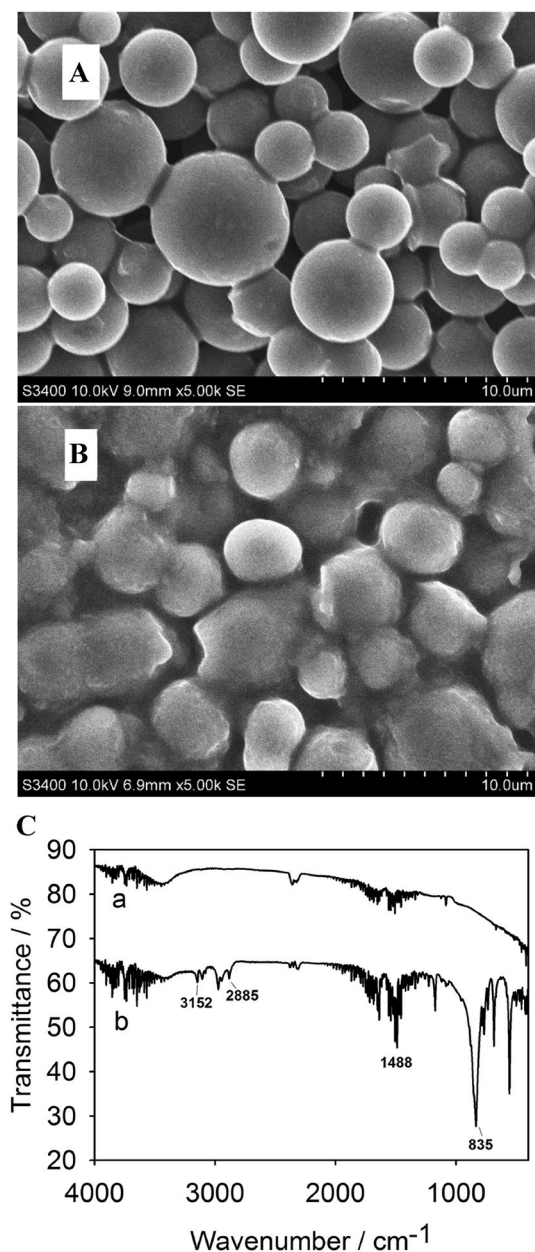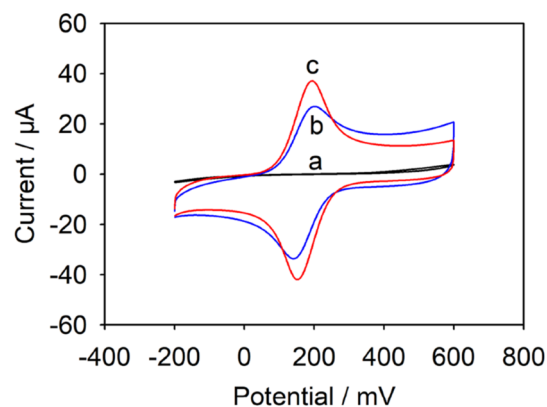
Fig. 2 CVs of **a** CPE; **b** CILE; and **c** GCILE in 1 mM Fe[(CN)$_6$]$^{3-/4-}$ and 0.1 M KCl solution, scan rate: 50 mV s^{-1}

Electrochemical behavior of SY and TZ

Figure 4 shows the DPVs of 10 µM SY and 30 µM TZ on different modified electrodes. As shown in the figure, two small separated oxidation peaks for SY and TZ could be observed at the traditional CPE (Curve a), and the currents were 0.414 µA and 0.742 µA, respectively. The oxidation peaks of SY and TZ on the CILE (Curve b) appeared at 0.652 V and 0.888 V, respectively. Their peak currents remarkably increased (about 53.64 µA for SY and about 18.36 µA for TZ). Compared with CILE, the oxidation peaks of SY and TZ on the GCILE (Curve c) shifted negatively (0.644 V for SY and 0.876 V for TZ), and peak currents further increased (73.89 µA for SY and 28.63 µA for TZ). This phenomenon may be attributed to that glassy carbon microspheres could provide more channels and show high electrocatalytic ability to SY and TZ. In addition, ionic liquid and glassy carbon microspheres combined through the CH-π interaction and promoted electron transfer rate synergistically.

Scan rate

The influence of scan rate on the current responses of SY and TZ was discussed using CV. Figure 5a, b shows CVs of 10 µM SY and 30 µM TZ with different scan rates from 25 and 350 mV s^{-1}, respectively. The anodic peak current increased linearly with scan rate, and the linear equations were described as: I(µA) = 0.4792 v (mV s^{-1})–3.0906 (r^2 = 0.9987) for SY, and I(µA) = 0.3829 v (mV s^{-1}) + 21.5952 (r^2 = 0.9909) for TZ, respectively, suggesting

Fig. 1 SEM images of **a** GCPE; **b** GCILE; **c** FT-IR spectra of GC **a** and GC-IL **b**

cm^2 s^{-1}) and the scan rate (V s^{-1}), respectively. The electroactive surface areas of CILE and GCILE were calculated to be 0.302 cm^2 and 0.673 cm^2, respectively. The results demonstrated that GCILE exhibited a larger electroactive surface area, providing more active sites for the analytes.
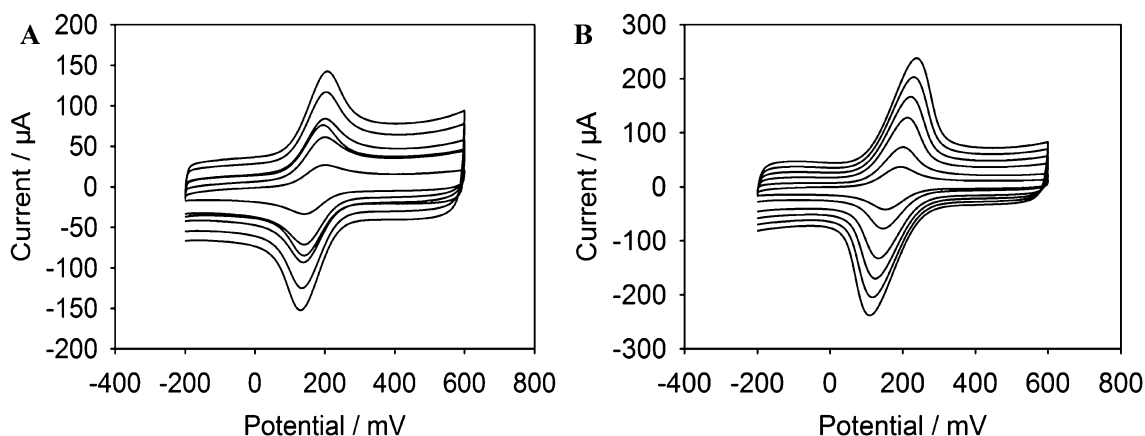
Fig. 3 CVs of **a** CILE and **b** GCILE with different scan rates in 1 mM $[Fe(CN)_6]^{3-/4-}$ and 0.1 M KCl solution, scan rates (from inner to outer): 50, 100, 150, 200, 250, 300 mV s^{-1}
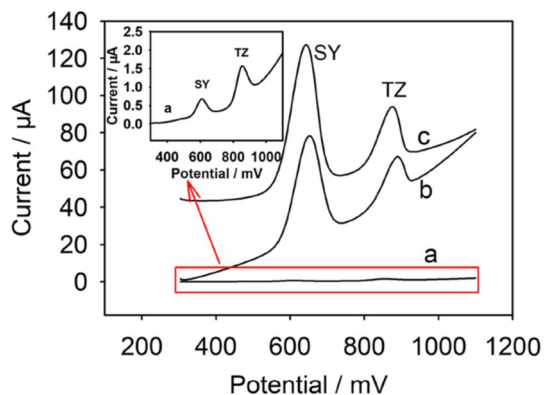

Fig. 4 DPVs of 10 μM SY and 30 μM TZ at **a** CPE; **b** CILE; and **c** GCILE in 0.1 M PBS (pH 7.0), the insert is an enlarged view of **a** CPE. Accumulation potential: 0.5 V, accumulation time: 150 s

the electrochemical reactions of SY and TZ at the modified electrode were both adsorption-controlled processes.

Effect of pH value

Figure 6 exhibits the effects of pH value on the current responses of SY and TZ. In the pH range of 4.0–9.0, the peak currents of SY and TZ increased until the pH value reached 7.0, then decreased when the pH value further increased. Thus, pH 7.0 was chosen for the subsequent studies.

In addition, the Epa of SY and TZ shifted linearly with pH values, and the linear equations were: E(V) = -0.0380 pH + 0.9107 ($r^2 = 0.9976$) for SY, and E(V) = -0.0391 pH + 1.1634 ($r^2 = 0.9938$) for TZ, respectively. The slopes
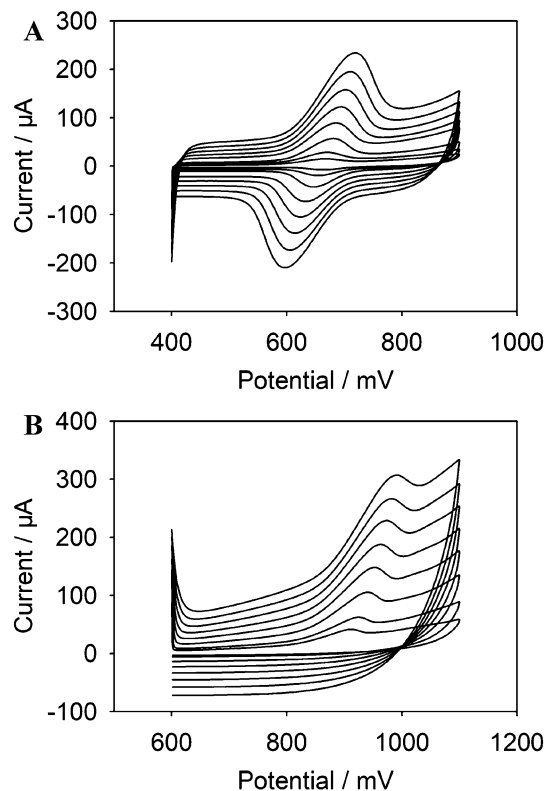

Fig. 5 CVs of 10 μM SY **a** and 30 μM TZ **b** on GCILE with different scan rates, scan rates (from inner to outer): 25, 50, 100, 150, 200, 250, 300, 350 mV s^{-1}

of -38.0 mV pH^{-1} and -39.1 mV pH^{-1} suggested that protons participated in the oxidation processes of SY and TZ on the GCILE, which was consistent with the previous literature
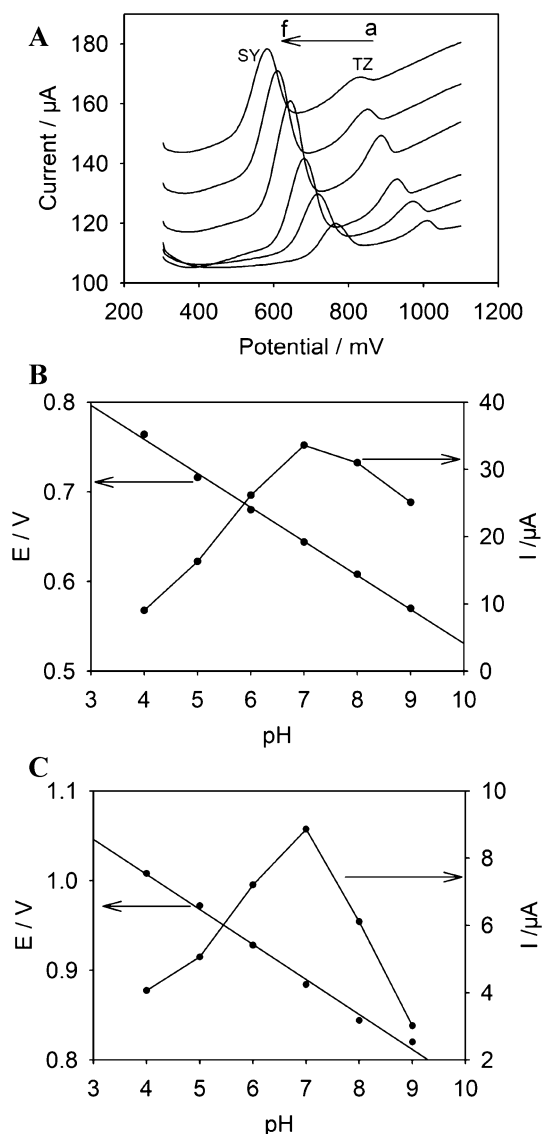
Fig. 6 **a** DPVs of 10 µM SY and 30 µM TZ on GCILE in different pH solutions (From a to f: pH 4, 5, 6, 7, 8, 9); **b** effects of pH value on the anodic peak current (Ipa) and potential (Epa) of 10 µM SY; **c** effects of pH value on the anodic peak current (Ipa) and potential (Epa) of 30 µM TZ

[19]. The possible mechanisms for the electrochemical processes of SY and TZ are described in Scheme 2.

Effect of composites composition

The influence of the proportion of glassy carbon microspheres and ionic liquid on the electrochemical responses for SY and TZ was also examined. As shown in Fig. 7,

the voltammetric responses of SY and TZ increased as the amount of glassy carbon microspheres increased. When the proportion of glassy carbon microspheres and ionic liquid was 1:1, SY and TZ exhibited two well-defined peaks at the modified electrode, and the voltammetric responses of SY and TZ reached the maximum. Then the further increase in the amount of glassy carbon microspheres, namely the decrease in the amount of highly conductive ionic liquid, resulted in a gradual decrease in voltammetric currents. A certain proportion of glassy carbon microspheres and ionic liquid can improve the conductivity of the sensor and the microstructure of the electrode surface, promoting electron transfer rate. However, more ionic liquid or glassy carbon microspheres will increase the background current of the modified electrode. Therefore, the proportion of glassy carbon microspheres and ionic liquid ($m_{GC}:m_{IL} = 1:1$) was utilized for the next experiments.

Effect of accumulation potential and accumulation time

Figure 8 displays the influence of accumulation potential on the voltammetric responses of SY and TZ. When the accumulation potential varied from 0.1 to 0.5 V, the current signals of SY and TZ both increased, and the current of SY increased more quickly than that of TZ. The voltammetric responses of SY and TZ both reached the maximum at 0.5 V. The further increase in the accumulation potential decreased the current responses of SY and TZ. Thus, we analyzed SY and TZ under the accumulation potential of 0.5 V.

As shown in Fig. 9, the current responses of SY and TZ gradually increased with the increasing accumulation time. After 150 s, the amounts of SY and TZ adsorbed on the sensor reached saturation, and the currents changed slightly. Therefore, the optimal accumulation time was 150 s.

Determination of SY and TZ

The analysis of SY and TZ was carried on GCILE using DPV. Figure 10 shows the DPVs of different concentrations of SY and TZ in 0.1 M PBS (pH 7.0). As shown in Fig. 10b, the oxidation peak current of SY linearly increased with the increase in the SY concentration in the range of 0.02–5 µM. The linear equation was: $I(\mu A) = 10.2050 \, c(\mu M) + 3.6288$ ($r^2 = 0.9946$), and the detection limit was found to be 0.01 µM (S/N = 3). In addition, the linear range of TZ was from 0.5 to 15 µM (shown in Fig. 10c) with a detection limit of 0.1 µM. The linear equation was: $I(\mu A) = 0.7810 \, c(\mu M) + 1.3336$ ($r^2 = 0.9921$).

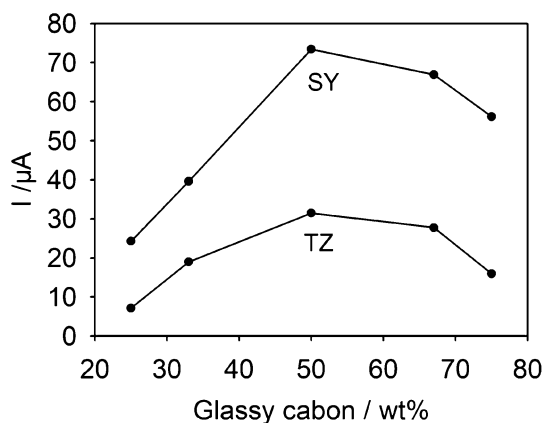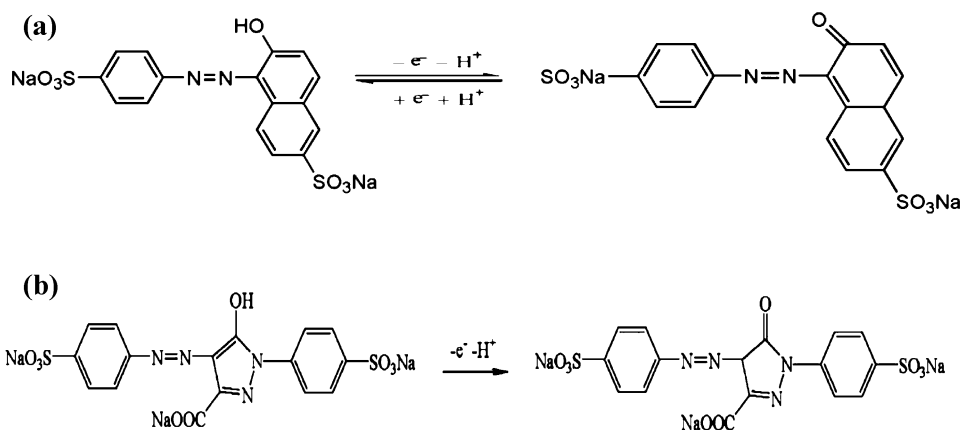**Scheme 2** Mechanisms for the electrochemical processes of SY **a** and TZ **b**

Fig. 7 Effect of different proportions of glassy carbon microspheres and ionic liquid on the anodic peak currents of 10 μM SY and 30 μM TZ
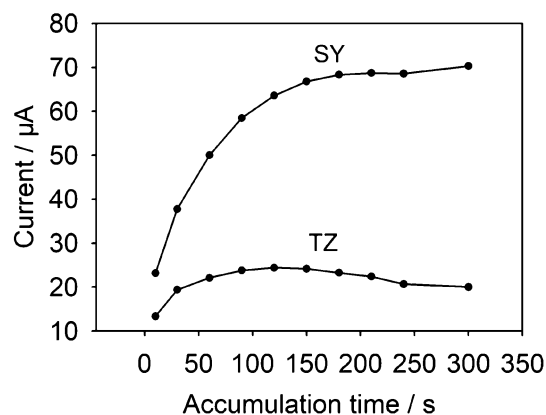

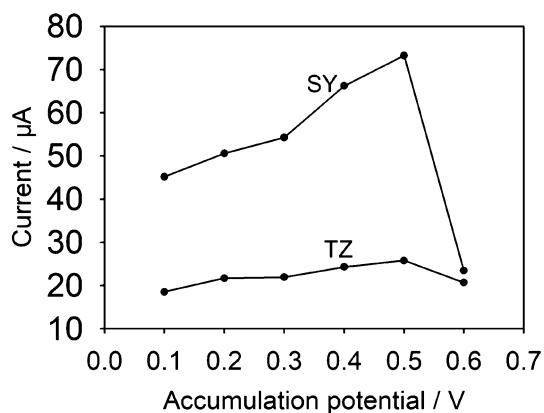**Fig. 9** Effect of accumulation time on the anodic peak current of 10 μM SY and 30 μM TZ

A comparison of the analytical parameters for SY and TZ at various modified electrodes is shown in Table 1. The results presented that the established method exhibited comparable or better linear ranges and detection limits than other previously reported methods [2, 20–25]. What is more, the proposed sensor had its unique advantages of simple preparation procedure, easily renewable surface, low cost, simple pretreatment, and antifouling ability.

The repeatability, stability, and anti-interference of the sensor

The relative standard deviations (RSD%) of 10 μM SY and 10 μM TZ for six measurements with the same GCILE were 2.17% and 3.72%, respectively. The RSD% of 3.43% and 4.89% were obtained for SY and TZ using six modified
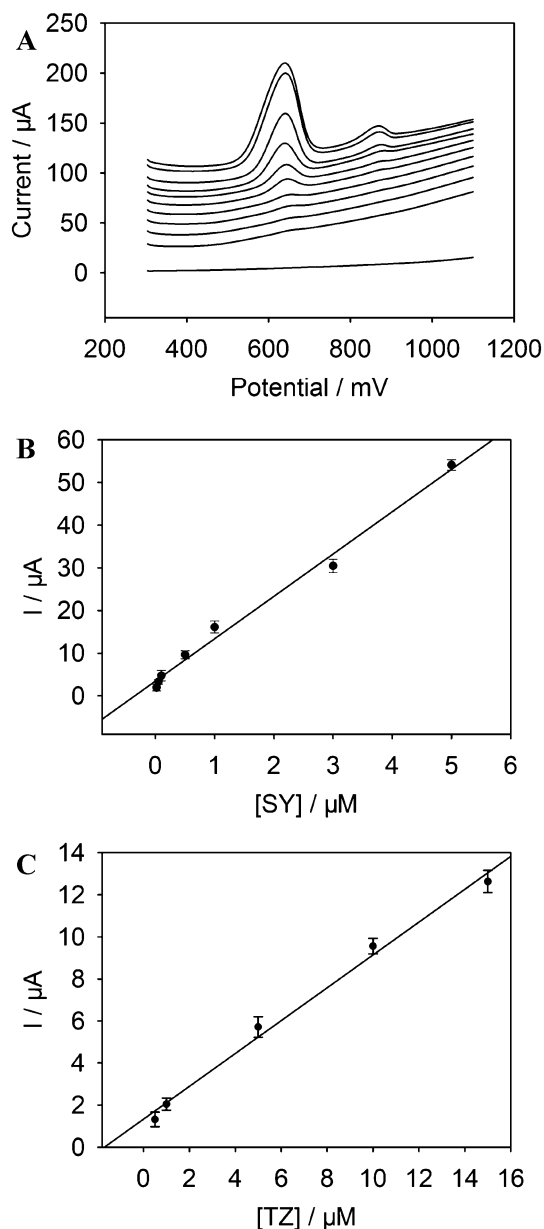

Fig. 8 Relationship between accumulation potential and the anodic peak current of 10 μM SY and 30 μM TZ

Fig. 10 **a** DPVs for different concentrations of SY and TZ on the GCILE (from bottom to upper: 0, 0.01, 0.02, 0.05, 0.1, 0.5, 1, 3, 5, 10, 15 μM); **b** relationship between the peak currents and the concentration of SY; **c** relationship between the peak currents and the concentration of TZ

electrodes prepared in the same process. The sensor was stored at room temperature for a month, and the modified electrode remained 93.8% and 94.5% of the initial response values for SY and TZ. The results exhibited that the sensor had good repeatability and stability.

The effect of interfering substances on the analysis of SY and TZ was studied. The analytical data indicated that 200-fold Na^+, Ca^{2+}, K^+, Cu^{2+}, Zn^{2+}, Cl^-, NO_3^-, 100-fold ascorbic acid, glycine, glucose, sucrose did not interfere with the measurement of SY and TZ, displaying that the suggested method exhibited excellent anti-interference ability.

Analytical applications

The sensor was utilized to the analysis of SY and TZ in beverages by using the standard addition method. Before determination, fruity soda (orange flavor) was ultrasonicated for 10 min to remove CO_2 and then diluted with 0.1 M PBS (pH 7.0). Orange juice and mango juice were directly diluted with PBS (pH 7.0) without sample pretreatment. Then appropriate amounts of these diluted samples were transferred to the electrochemical cell for the detection of SY and TZ by the presented method. The recovery experiments were carried out to verify the accuracy of the proposed method, and good recoveries for food colorants (92.0–96.0% for SY and 102.0–106.0 for TZ) were obtained. To further validate the method, the HPLC method was employed for comparison purposes. The results are presented in Table S1. The results obtained in this work agreed well with those acquired by the reference HPLC method, which suggested that the proposed method had good promising application.

Conclusions

In this work, a 1-butylpyridinium hexafluorophosphate@ glassy carbon microspheres composites electrode was developed in a simply fabricated procedure. The anodic peaks of SY and TZ were distinctly separated at the modified electrode, and they could be simultaneously analyzed with good selectivity and negligible interaction. Under the optimized conditions, the sensor exhibited improved electrocatalytic

Table 1 Comparison of the analytical performance of the different modified electrodes for determination of SY and TZ

Modified electrode	Method	Analyte	Linear range (μM)	Detection limit (μM)	Sample analyzed	Reference
Nd_{OX}[a]/CPE[b]	SWV[i]	SY	0.20–2.0	0.09	Orange juice; tangerine juice powder; pharmaceutical dosage	[2]
		TZ	0.05–2.5	0.02		
MWCNTs[c]–IL[d]/CCE[e]	DPV[j]	SY	0.4–110	0.1	Powdered orange juice; orange juice; beverage	[20]
		TZ	3–70	1.1		
MWCNTs/GCE[f]	DPV	SY	0.55–7.0	0.12	Sample A/B/C (unspecified type)	[21]
		TZ	1.0–7.0	0.22		
PLPA[g]/GCE	DPV	SY	0.4–14.0	0.04	Soft drinks; juice powder; Sugar-coated tablets	[22]
		TZ	0.4–165.0	0.02		
ZnO/cysteic acid/GCE	DPV	SY	0.1–3.0	0.03	Orange juice; fruit juice; peach gelatin	[23]
		TZ	0.07–1.86	0.01		
CuS microflowers/ GCE	DPV	SY	0.1–700	0.006	Mirinda; jelly; candy	[24]
		TZ	0.4–100	0.012		
Graphene/ IL/CCE	DPV	SY	0.1–15	0.073	Powdered orange juice; orange juice; beverage	[25]
		TZ	0.1–20	0.081		
GCILE[h]	DPV	SY	0.02–5	0.01	Orange juice; fruity soda; mango juice	This work
		TZ	0.5–15	0.1		

[a]Nd_{OX}: Nd_2O_3

[b]CPE: carbon paste electrode

[c]MWCNTs: multi-walled carbon nanotubes

[d]IL: ionic liquid

[e]CCE: carbon–ceramic electrode

[f]GCE: glassy carbon electrode

[g]PLPA: poly(L-phenylalanine)

[h]GCILE: glassy carbon microspheres ionic liquid composite electrode

[i]SWV: square wave voltammetry

[j]DPV: differential pulse voltammetry

activity toward SY and TZ. The method was successfully established to detect SY and TZ in beverages simultaneously.

References

1. S. Asaadi, R. Hajian, DNA binding studies of Sunset Yellow FCF using spectroscopy, viscometry and electrochemical techniques. J. Mol. Struct. **1146**, 861–867 (2017)
2. K. Marquez-Mariño, J. Penagos-Llanos, O. García-Beltrán, E. Nagles, J.J. Hurtado, Development of a novel electrochemical sensor based on a carbon paste electrode decorated with Nd_2O_3 for the simultaneous detection of tartrazine and sunset yellow. Electroanalysis **30**, 2760–2767 (2018)
3. S.C. Sun, B.C. Hsieh, M.C. Chuang, Electropolymerised-hemincatalysed reduction and analysis of tartrazine and sunset yellow. Electrochim. Acta **319**, 766–774 (2019)
4. M. Vidal, R. Garcia-Arrona, A. Bordagaray, M. Ostra, G. Albizu, Simultaneous determination of color additives tartrazine and allura red in food products by digital image analysis. Talanta **184**, 58–64 (2018)
5. E. Heidarizadi, R. Tabaraki, Simultaneous spectrophotometric determination of synthetic dyes in food samples after cloud point extraction using multiple response optimizations. Talanta **148**, 237–246 (2016)
6. T.T. Zou, P.L. He, A. Yasen, Z. Li, Determination of seven synthetic dyes in animal feeds and meat by high performance liquid chromatography with diode array and tandem mass detectors. Food Chem. **138**, 1742–1748 (2013)
7. F.I.D. Andrade, M.I.F. Guedes, Í.G.P. Vieira, F.N.P. Mendes, P.A.S. Rodrigues, C.S.C. Maia, Determination of synthetic food dyes in commercial soft drinks by TLC and ion-pair HPLC. Food Chem. **157**, 193–198 (2014)
8. M. Ryvolová, P. Táborský, P. Vrábel, P. Krásenský, J. Preisler, Sensitive determination of erythrosine and other red food colorants using capillary electrophoresis with laser-induced fluorescence detection. J. Chromatogr. A **1141**, 206–211 (2007)
9. P. Sierra-Rosales, C. Toledo-Neira, J.A. Squella, Electrochemical determination of food colorants in soft drinks using MWCNT-modified GCEs. Sensors Actuat. B **240**, 1257–1264 (2017)
10. X.L. Qiu, L.M. Lu, J. Leng, Y.F. Yu, W.M. Wang, M. Jiang, An enhanced electrochemical platform based on graphene oxide and multi-walled carbon nanotubes nanocomposite for sensitive determination of sunset yellow and tartrazine. Food Chem. **190**, 889–895 (2016)

11. D.M. Stanković, S. Škrivanj, N. Savić, A.S. Nikolić, P. Vulić, D.D. Manojlović, Application of novel Zn-ferrite modified glassy carbon paste electrode as a sensor for determination of Cd(II) in waste water. Electroanalysis **26**, 1536–1543 (2014)

12. M. Keyvanfard, N. Najjarian, K. Alizad, Electrocatalytic determination of penicillamine using multiwall carbon nanotubes paste electrode and chlorpromazine as a mediator. J. Anal. Chem. **72**, 1045–1050 (2017)

13. S.Z. Mohammadi, H. Beitollahi, N.M. Rahimi, Voltammetric determination of epinephrine and uric acid using modified graphene oxide nano sheets paste electrode. J. Anal. Chem. **74**, 345–354 (2019)

14. S. Motoc, F. Manea, C. Orha, A. Pop, Enhanced electrochemical response of diclofenac at a fullerene-carbon nanofiber paste electrode. Sensors **19**, 1332 (2019)

15. Y.H. Li, Y. Ji, B.B. Ren, L.N. Jia, Q. Cai, X.S. Liu, Palladium-doped graphene-modified nanocarbon ionic liquid electrode: preparation, characterization and simultaneous voltammetric determination of dopamine and uric acid. J. Iran. Chem. Soc. **16**, 1903–1912 (2019)

16. T. Ören, Ü. Anık, Voltammetric determination of caffeine by using gold nanoparticle-glassy carbon paste composite electrode. Measurement **106**, 26–30 (2017)

17. H. Dai, H.F. Xu, X.P. Wu, Y.W. Chi, G.N. Chen, Fabrication of a new electrochemiluminescent sensor for fentanyl citrate based on glassy carbon microspheres and ionic liquid composite paste electrode. Anal. Chim. Acta **647**, 60–65 (2009)

18. F. Shahdost-fard, M. Roushani, The use of a signal amplification strategy for the fabrication of a TNT impedimetric nanoaptasensor based on electrodeposited NiONPs immobilized onto a GCE surface. Sensor. Actuat. B **246**, 848–853 (2017)

19. J.H. Wu, H.L. Lee, Determination of sunset yellow and tartrazine in drinks using screen-printed carbon electrodes modified with reduced graphene oxide and NiBTC framework. Microchem. J. **158**, 105133 (2020)

20. M.R. Majidi, R.F.B. Baj, A. Naseri, Carbon nanotube-ionic liquid (CNT-IL) nanocomposite modified sol-gel derived carbon-ceramic electrode for simultaneous determination of sunset yellow and tartrazine in food samples. Food Anal. Method. **6**, 1388–1397 (2013)

21. P. Sierra-Rosales, C. Toledo-Neira, J.A. Squella, Electrochemical determination of food colorants in soft drinks using MWCNT-modified GCEs. Sensor. Actuat. B **240**, 1257–1264 (2017)

22. M.Y. Chao, X.Y. Ma, Convenient electrochemical determination of sunset yellow and tartrazine in food samples using a poly(L-phenylalanine)-modified glassy carbon electrode. Food Anal. Method. **8**, 130–138 (2015)

23. P.S. Dorraji, F. Jalali, Electrochemical fabrication of a novel ZnO/cysteic acid nanocomposite modified electrode and its application to simultaneous determination of sunset yellow and tartrazine. Food Chem. **227**, 73–77 (2017)

24. J. Li, M.Q. Liu, J.B. Jiang, B.B. Liu, H.X. Tong, Z.F. Xu, Morphology-controlled electrochemical sensing properties of CuS crystals for tartrazine and sunset yellow. Sensor. Actuat. B **288**, 552–563 (2019)

25. M.R. Majidi, M.H. Pournaghi-Azar, R.F.B. Baj, A. Naseri, Formation of graphene nanoplatelet-like structures on carbon-ceramic electrode surface: application for simultaneous determination of sunset yellow and tartrazine in some food samples. Ionics **21**, 863–875 (2015)